Far-Infrared Conductivity Measurements of Pair Breaking in Superconducting $Nb_{0.5}Ti_{0.5}N$ Thin Films Induced by an External Magnetic Field

Xiaoxiang Xi,[1] J. Hwang,[1,2] C. Martin,[1] D. B. Tanner,[1] and G. L. Carr[3]
[1]*Department of Physics, University of Florida, Gainesville, Florida 32611, USA*
[2]*Department of Physics, Pusan National University, Busan 609-735, Republic of Korea*
[3]*National Synchrotron Light Source, Brookhaven National Laboratory, Upton, New York 11973, USA*
(Received 16 August 2010; published 16 December 2010)

We report the complex optical conductivity of a superconducting thin film of $Nb_{0.5}Ti_{0.5}N$ in an external magnetic field. The field was applied parallel to the film surface and the conductivity extracted from far-infrared transmission and reflection measurements. The real part shows the superconducting gap, which we observe to be suppressed by the applied magnetic field. We compare our results with the pair-breaking theory of Abrikosov and Gor'kov and confirm directly the theory's validity for the optical conductivity.

DOI: 10.1103/PhysRevLett.105.257006 PACS numbers: 74.78.−w, 74.25.Ha, 78.20.−e, 78.30.−j

Magnetic fields have dramatic effects on superconductors; when they are stronger than the upper critical field, superconductivity is destroyed. Fields below this critical value induce supercurrents and also act on the spin and orbital motion of quasiparticles. An applied field lifts the spin degeneracy of each electronic state, potentially causing a paramagnetic shift of the quasiparticle density of states [1], which would give a linear shift of the spectroscopic gap with field [2]. The effect is noticeable only for materials with small spin-orbit scattering, in which the spin is a "good" quantum number. The field also alters the orbitals of single-particle states from which the BCS ground state is formed, breaking the time-reversal symmetry of the condensate. The result is a finite pair breaking and an overall weakening of the superconducting state. This weakening is directly revealed by a reduction in the single-particle gap and forms the basis of the pair-breaking theory originally proposed by Abrikosov and Gor'kov [3] to describe the effect of magnetic impurities on superconductivity. The depairing phenomena can be characterized by a single pair-breaking parameter Γ that depends on whether the theory describes external magnetic fields, supercurrents, spin exchange, or other effects. Maki [4] showed that a thin superconductor in the dirty limit will exhibit pair breaking, equivalent to that caused by magnetic impurities, when subjected to a homogeneous magnetic field. Because paramagnetism and pair breaking can both affect the spectroscopic gap, experimental verification of the pair-breaking effect is simplified in materials with large spin-orbit scattering [5].

Ordinary metallic superconductors have a gap in their optical spectrum [6], requiring a minimum of 2Δ of photon energy to break Cooper pairs. The gap, which in weak coupling BCS theory is $2\Delta \simeq 3.5kT_c$, makes the $T = 0$ real part of the optical conductivity be zero for photon energies below the gap. The missing spectral weight in $\sigma_1(\omega)$ appears as a delta function at zero frequency [7]. By the Kramers-Kronig relations, the delta function gives a dominant $1/\omega$ form to $\sigma_2(\omega)$ and is responsible for the frequency-independent penetration depth $\lambda_L = c/\sqrt{4\pi\omega\sigma_2}$. This behavior is observed in most metallic superconductors (Sn, In, Pb, Hg, etc.) although strong-coupling effects are sometimes necessary for quantitative agreement [8]. By determining both the real and imaginary parts of the optical conductivity under an applied magnetic field, one can test theories for the magnetic field suppression of the gap.

We find it somewhat surprising that magnetic-field-induced pair-breaking effects have not been convincingly verified by optical studies. Such effects have been observed in tunneling spectra [9] and are hinted at by absorption data [2]. In addition, the effects of magnetic impurities have been studied in detail [10]. In this Letter, we report far-infrared transmission and reflection spectra of $Nb_{0.5}Ti_{0.5}N$ under an external magnetic field, applied parallel to the film surface. The extracted optical conductivity σ_1 demonstrates a suppression of the gap by the field, in quantitative agreement with the pair-breaking theory. This is the first time that optical absorption has been employed to test quantitatively the theory of pair breaking by an external magnetic field.

We selected for study a 10-nm-thick film on quartz from a set of NbTiN thin films of varying thicknesses and substrate materials. A selection criterion was strong spin-orbit scattering $\hbar/\tau_{so}\Delta \gg 1$ [5], where the spin-orbit scattering time $\tau_{so} = 3.0 \times 10^{-14}$ s is taken to be that of NbTi [11] and Δ is the single-particle gap. The films were grown by reactive magnetron sputtering in argon and nitrogen gas with a NbTi cathode [12]. Transmittance data (inset in the upper panel in Fig. 1) give the normal-state sheet resistance: $R_\square = 146\ \Omega/\square$. Magnetic susceptibility measurements with a SQUID magnetometer determine $T_c \approx 12$ K and $H_{c2}^{\parallel} \approx 15$ T. The optical gap for $T = 2$ K ($\ll T_c$) and zero field is 28.5 cm^{-1}. The quartz substrate has negligible absorption in the spectral range of interest (10–110 cm^{-1}). Infrared transmission and reflection measurements were

 © 2010 The American Physical Society

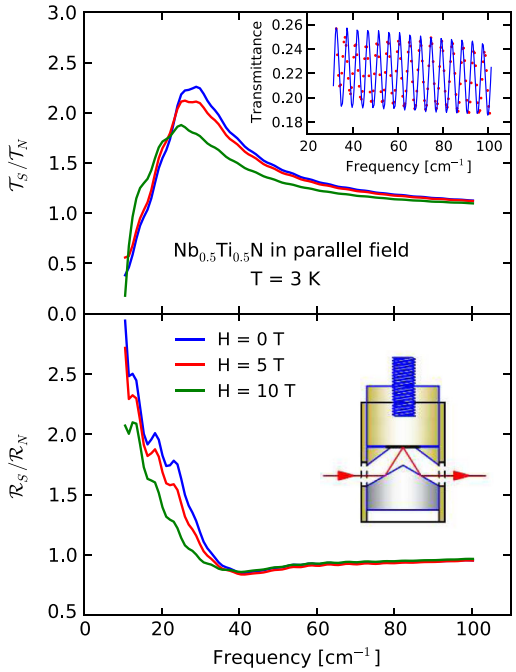

FIG. 1 (color online). Superconducting to normal-state transmission (upper panel) and reflection (lower panel) ratios at 0, 5, and 10 T. The weak oscillatory features are partially resolved multiple internal reflections in the substrate. The upper panel inset is the transmittance for $T = 300$ K, measured at 3× higher spectral resolution along with a fit using the optical constants of quartz [13] (blue curve). The inset in the lower panel is a diagram of the reflection sample holder. The sample is the thin black slab near the middle. A polished aluminum roof-type mirror reflects the input beam onto the sample at a 30° angle and then redirects the reflected beam back onto the original optical path.

performed at Beam line U4IR of the National Synchrotron Light Source, Brookhaven National Laboratory. The samples were mounted in a ^{4}He Oxford cryostat equipped with a 10 T superconducting magnet; the minimum temperature is 1.6 K. The spectra were collected by using a Bruker IFS 66-v/S spectrometer and a high-sensitivity, large-area, *B*-doped Si composite bolometer operating at 1.8 K; cooled filters limited the upper frequency to 110 cm^{-1}.

A sketch of the reflection stage is shown in the inset in the lower panel in Fig. 1. The angle of incidence for the reflection measurements is about 30°; for transmission it is near normal. The magnetic field is applied parallel to the film surface. The field direction is important when considering the behavior of these type-II superconductors. For a normal field, vortices appear above H_{c1} and form a dense lattice of lossy core material as it approaches H_{c2}. We avoided this vortex regime by orienting the field parallel to the film surface. The machining tolerances are such that the misalignment is less than 0.3°, making the number of vortices be 0.5% of those in a perpendicular field. In this case, because the thickness is much smaller than the penetration depth and somewhat smaller than the coherence length, a significant density of vortices is unlikely. $Nb_{1-x}Ti_xN$ typically has a penetration depth $\lambda \approx 100$ nm and a coherence length $\xi \approx 20$ nm [14], satisfying $\kappa \equiv \lambda/\xi \gg 1$. When a magnetic field is applied parallel to the film surface, the vortex spacing is greater than ξ [15], which itself is close to the film thickness. Therefore we do not expect vortex-induced effects to be significant. Moreover, the field decays according to the much larger penetration depth, making the average field in the film be approximately 0.999 of the applied field [16] and, hence, nearly uniform.

Our goal is to extract the optical conductivity of the thin-film superconductor from reflection and transmission measurements. Beginning with the pioneering work of Palmer and Tinkham [8], this approach has been used a number of times to study both metallic and cuprate superconductors [17]. In a conventional transmittance or reflectance measurement, one measures separately the sample and a reference having known optical properties—typically, an open aperture with no sample for transmittance and a known metal for reflectance. Sample exchange can lead to errors, especially for the absolute reflection, where sample orientation is critical. To avoid sample exchange errors, we used the sample in the normal state, and at $H = 0$ T, for our reference. Specifically, we measured the sample spectrum (transmission or reflection) at different fields ranging from 0 to 10 T in the superconducting state ($T = 3$ K), using the normal-state ($T = 20$ K), zero-field spectrum for the reference. If required, the relative measurements can be made absolute by measuring the normal-state transmittance and reflectance or by calculating them from the Drude model in the limit $\omega \ll 1/\tau$ (a very good assumption for our films). The directly acquired data are therefore the ratios of transmittance $\mathcal{T}_S/\mathcal{T}_N$ and reflectance $\mathcal{R}_S/\mathcal{R}_N$, where the subscripts S and N denote superconducting state and normal state, respectively. Figure 1 shows the data at zero, intermediate, and high fields, measured with a resolution of 3.5 cm^{-1}, which does not fully resolve the interference fringes from multiple reflections inside the substrate. The peak in $\mathcal{T}_S/\mathcal{T}_N$ shifts to lower frequency as the field increases, suggesting the suppression of the energy gap due to the field. The reflection data were corrected for the measured stray light and for the 30° angle of incidence (see [18]) before calculating the optical conductivity. The field-dependent transmittance is similar to recent data for NbN measured at a single frequency [19].

The analysis for the thin-film optical conductivity $\sigma = \sigma_1 + i\sigma_2$ begins with the expressions for the normal-incidence transmission through, and reflection from, the front film surface of the sample [8]:

$$\mathcal{T}_f = \frac{4n}{(Z_0\sigma_1 d + n + 1)^2 + (Z_0\sigma_2 d)^2}, \quad (1)$$

$$\mathcal{R}_f = \frac{(Z_0\sigma_1 d + n - 1)^2 + (Z_0\sigma_2 d)^2}{(Z_0\sigma_1 d + n + 1)^2 + (Z_0\sigma_2 d)^2}, \quad (2)$$

where $Z_0 \approx 377\ \Omega$ is the vacuum impedance, d is the film thickness, and σ_1 and σ_2 are the real and imaginary parts of

the optical conductivity of the thin film, either in the superconducting state or in the normal state. In practice, we measure the combination of film and substrate, giving the external transmittance $\mathcal{T}_{\rm ext}$ and external reflectance $\mathcal{R}_{\rm ext}$. If the substrate surfaces are parallel on the scale of the wavelength and the measurement resolution is high enough, these quantities typically show fringes due to partially coherent multiple internal reflections inside the substrate. Smoothing high resolution data or taking measurements with a low resolution produces the incoherent spectrum, where one may add intensities rather than amplitudes. In this case, $\mathcal{T}_{\rm ext} = \mathcal{T}_f(1-\mathcal{R}_Q)e^{-\alpha x}/(1-\mathcal{R}_Q\mathcal{R}'_f e^{-2\alpha x})$, where $\mathcal{R}_Q \approx (n-1)^2/(n+1)^2$ is the reflectance of the quartz surface, α is the (small) absorption coefficient of the quartz, x is the thickness of the quartz, and $\mathcal{R}'_f$ is the film reflection from inside the substrate. There is a similar equation for $\mathcal{R}_{\rm ext}$. Quartz has negligible absorption and dispersion over the spectral and temperature range of interest. Thus we take $\alpha = 0$ and $n = 2.12$, yielding $\mathcal{R}_Q \approx 0.13$.

Our measurements give us the external transmission and reflection ratios $\mathcal{T}_{{\rm ext},S}/\mathcal{T}_{{\rm ext},N}$ and $\mathcal{R}_{{\rm ext},S}/\mathcal{R}_{{\rm ext},N}$, respectively, that include the substrate. For the range of conductivity values expected for the film, we find that, to a very good approximation, $\mathcal{T}_{{\rm ext},S}/\mathcal{T}_{{\rm ext},N} = \mathcal{T}_S/\mathcal{T}_N$ and $\mathcal{R}_{{\rm ext},S}/\mathcal{R}_{{\rm ext},N} = \mathcal{R}_S/\mathcal{R}_N$. The normal-state transmittance and reflectance can be derived from Eqs. (1) and (2) by setting $\sigma_1 = \sigma_N$, $\sigma_2 = 0$, $\mathcal{T}_N = 4n/(Z_0\sigma_N d + n + 1)^2$, and $\mathcal{R}_N = (Z_0\sigma_N d + n - 1)^2/(Z_0\sigma_N d + n + 1)^2$. Here σ_N is related to the normal-state sheet resistance of the thin film $R_\square = 1/\sigma_N d$, which we have determined from the normal-state transmittance. Hence we know $\mathcal{T}_N$ and $\mathcal{R}_N$ and may use them to calculate $\mathcal{T}_S$ and $\mathcal{R}_S$ from our measured ratios. Then we invert Eqs. (1) and (2) to find

$$\frac{\sigma_1}{\sigma_N} = \frac{nR_\square}{Z_0}\frac{1-\mathcal{R}_S-\mathcal{T}_S}{\mathcal{T}_S}, \tag{3}$$

$$\frac{\sigma_2}{\sigma_N} = \frac{R_\square}{Z_0}\left[\frac{4n}{\mathcal{T}_S} - (Z_0\sigma_1 d + n + 1)^2\right]^{1/2}. \tag{4}$$

The normalized optical conductivity at 0, 5, and 10 T are shown in Figs. 2(a)–2(c). σ_2/σ_N has some data points missing because the term under the square root in Eq. (4) is not guaranteed to be positive for the measured transmission and reflection when noise is included. A weak interference fringe in both the transmission and reflection measurements results in the excess σ_2/σ_N over the 40–80 cm^{-1} range. The solid lines are fits to the data using the pair-breaking theory as extended by Skalski *et al.* [20] to calculate σ_1/σ_N at 0 K:

$$\frac{\sigma_1}{\sigma_N} = \frac{1}{\omega}\int_{\Omega_G-\omega/2}^{-\Omega_G+\omega/2} dq[n(q+\omega/2)n(q-\omega/2) + m(q+\omega/2)m(q-\omega/2)] \tag{5}$$

for $\omega \geq 2\Omega_G$ and zero otherwise, where $n(q) = {\rm Re}(u/\sqrt{u^2-1})$ and $m(q) = {\rm Re}(1/\sqrt{u^2-1})$. u is the solution to $u\Delta = q + i\Gamma u/\sqrt{u^2-1}$, with Δ the pair-correlation gap. This, in turn, can be determined from the pair-breaking parameter Γ and the zero-field excitation gap Δ_0 by using $\ln(\Delta/\Delta_0) = -\pi\Gamma/4\Delta$ for $\Gamma < \Delta$. Ω_G in the integration limits is the effective spectroscopic gap: $\Omega_G = \Delta[1-(\Gamma/\Delta)^{2/3}]^{3/2}$ for $\Gamma < \Delta$. We fit our $H = 0$ T results to determine Δ_0 and then proceeded to fit σ_1/σ_N for $H > 0$ T by using only Γ as an adjustable parameter. The imaginary part of the conductivity (dashed lines) was calculated by a Kramers-Kronig transform of the real part. The temperature $T \approx 0.25T_c$ is low enough that the gap has reached its zero-temperature value. The zero-field case reduces to the standard BCS Mattis-Bardeen [6] description of a dirty-limit superconductor, consistent with results for the similar compound NbN [21]. Figure 2(d) shows the fitted σ_1/σ_N at six different fields. Clearly, the absorption edge moves to lower energy as the field increases. The field-induced pair breaking also smears out the gap-edge singularity in the quasiparticle density of states [20], so that the initial rise of σ_1 becomes less abrupt for increasing fields, as can be seen by comparing the 0 T and the 10 T results in Fig. 2.

The oscillator-strength sum rule $\int_0^\infty \sigma_1(\omega)d\omega = \pi n e^2/2m$, where n is the electron density and e and m are the charge and mass of the electron, respectively, requires the area under $\sigma_1(\omega)$ to be the same for normal and superconducting states. The ratio σ_1/σ_N in Fig. 2 is always less than unity; the "missing area" condenses to a

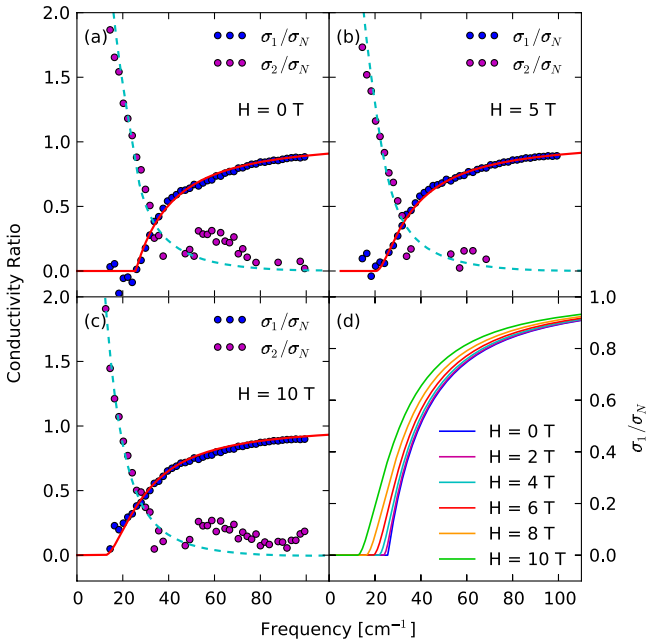

FIG. 2 (color online). (a)–(c) The real and imaginary parts of the $T = 3$ K superconducting state optical conductivity (normalized to the normal-state conductivity) at three different applied magnetic fields. The solid lines are fits to σ_1/σ_N using the pair-breaking theory. The dashed lines show the corresponding σ_2/σ_N as determined by a Kramers-Kronig transform of the real part. (d) The fitted σ_1/σ_N at six fields.

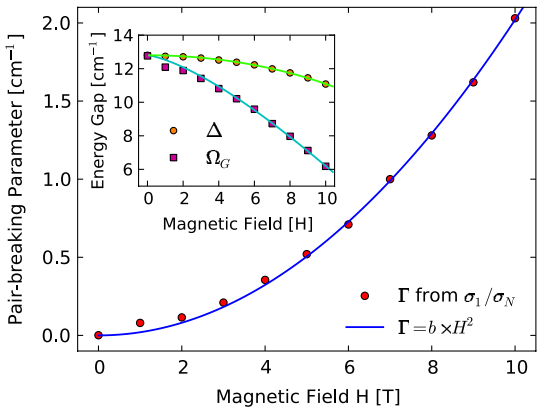

FIG. 3 (color online). Field dependence of the pair-breaking parameter Γ, determined from the experimental optical conductivity (circles) along with a fit to $\Gamma = bH^2$ (solid line). The inset shows the pair-correlation gap Δ and the effective spectroscopic gap Ω_G vs field. The solid lines are theoretical predictions using the pair-breaking theory and the fitted value of b.

δ function at zero frequency that is a measure of pair condensate density and is directly related to the pair-correlation gap. Figure 2(d) therefore shows a weakening of superconductivity as the field increases. There is a limit in which the absorption edge approaches 0, while the missing area remains finite. The superconductor enters a "gapless" region but still maintains superconducting properties.

The quantity Γ describes the strength of pair breaking. For any perturbing Hamiltonian that breaks time-reversal symmetry, Γ is proportional to the square of the perturbing Hamiltonian in the dirty limit [22]. For the range of fields used here, Γ is quadratic in the field: $\Gamma = bH^2 = \tau_{\rm tr} v_f^2 (eHd)^2/18$, where $\tau_{\rm tr}$ is the transport collision time and d is the film thickness [15]. Γ, as extracted from our data at different fields, is plotted in Fig. 3. The quadratic fit is good, yielding $b = 0.020$ cm^{-1}/T^2. We estimate $\tau_{\rm tr}$ from $\sigma_N = ne^2\tau_{\rm tr}/m$ and $R_\square = 1/\sigma_N d$, $\tau_{\rm tr} = m/R_\square dne^2 \approx 1.51 \times 10^{-16}$ s, where $R_\square = 146\ \Omega/\square$, $d = 10$ nm, and $n \approx 1.61 \times 10^{23}$ cm^{-3} is the electron density of NbN [23] similar to that of NbTiN. If we take the Fermi velocity to be that of NbN [23], $v_f \approx 1.95 \times 10^8$ cm/s, then $b = 0.039$ cm^{-1}/T^2, consistent with the fitted value within the uncertainty of the materials parameters.

The spectroscopic energy gap Ω_G and the pair-correlation gap Δ are shown in the inset in Fig. 3. Both Ω_G and Δ drop as the field increases, but the reduction of Ω_G is much greater at any given field. The sample at the highest attainable field of 10 T is still far away from the gapless region where Ω_G vanishes. The experimental and theoretical values of Ω_G and the pair-correlation gap Δ are in excellent agreement.

In conclusion, we measured far-infrared transmission and reflection of a thin-film superconductor in a magnetic field parallel to the film surface. The real and imaginary parts of the optical conductivity are derived from these data, the former showing the absorption edge depressed due to the applied in-plane field. The degree of suppression is in good agreement with the pair-breaking theory.

This work was supported by U.S. Department of Energy through DE-ACO2-98CH10886 (NSLS) and DE-FG02-02ER45984 (University of Florida) and by Korea NRF No. 20090074977. We are grateful to P. J. Hirschfeld for valuable discussions and to G. Nintzel for technical support. We thank P. Bosland and E. Jacques for providing the NbTiN samples.

[1] R. Meservey, P. M. Tedrow, and P. Fulde, Phys. Rev. Lett. **25**, 1270 (1970).
[2] P. J. M. van Bentum and P. Wyder, Phys. Rev. B **34**, 1582 (1986).
[3] A. A. Abrikosov and L. P. Gor'kov, Zh. Eksp. Teor. Fiz. **39**, 1781 (1960); Sov. Phys. JETP **12**, 1243 (1961).
[4] K. Maki, Prog. Theor. Phys. **29**, 603 (1963).
[5] R. C. Bruno and B. B. Schwartz, Phys. Rev. B **8**, 3161 (1973); R. Meservey, P. M. Tedrow, and R. C. Bruno, *ibid.* **11**, 4224 (1975).
[6] D. C. Mattis and J. Bardeen, Phys. Rev. **111**, 412 (1958).
[7] M. Tinkham and R. A. Ferrell, Phys. Rev. Lett. **2**, 331 (1959).
[8] R. E. Glover and M. Tinkham, Phys. Rev. **104**, 844 (1956); **108**, 243 (1957); L. H. Palmer and M. Tinkham, *ibid.* **165**, 588 (1968); D. M. Ginsberg, P. L. Richards, and M. Tinkham, Phys. Rev. Lett. **3**, 337 (1959); H. D. Drew and A. J. Sievers, *ibid.* **19**, 697 (1967).
[9] A. Anthore, H. Pothier, and D. Esteve, Phys. Rev. Lett. **90**, 127001 (2003).
[10] G. J. Dick and F. Reif, Phys. Rev. **181**, 774 (1969); P. B. Littlewood, C. M. Varma, and E. Abrahams, J. Low Temp. Phys. **95**, 83 (1994).
[11] R. R. Hake, Appl. Phys. Lett. **10**, 189 (1967).
[12] P. Bosland *et al.*, in *Proceedings of the Sixth Workshop on RF Superconductivity, Virginia, 1993*, edited by R. M. Sundelin (Gordon and Breach, New York, 1994).
[13] E. V. Loewenstein, D. R. Smith, and R. L. Morgan, Appl. Opt. **12**, 398 (1973).
[14] L. Yu, N. Newman, and J. Rowell, IEEE Trans. Appl. Supercond. **12**, 1795 (2002); L. Yu *et al.*, *ibid.* **15**, 44 (2005).
[15] *Superconductivity*, edited by R. D. Parks (Marcel Dekker, New York, 1969), Vol. 2, pp. 837 and 1073.
[16] M. Tinkham, *Introduction to Superconductivity* (McGraw-Hill, New York, 1996).
[17] F. Gao *et al.*, Phys. Rev. B **43**, 10 383 (1991); H. Tashiro *et al.*, *ibid.* **78**, 014509 (2008).
[18] See supplementary material at http://link.aps.org/supplemental/10.1103/PhysRevLett.105.257006 for a detailed description of the corrections.
[19] M. Šindler *et al.*, Phys. Rev. B **81**, 184529 (2010).
[20] S. Skalski, O. Betbeder-Matibet, and P. R. Weiss, Phys. Rev. **136**, A1500 (1964); J. L. Levine, *ibid.* **155**, 373 (1967).
[21] K. E. Kornelsen *et al.*, Phys. Rev. B **44**, 11 882 (1991); H. S. Somal *et al.*, Phys. Rev. Lett. **76**, 1525 (1996).
[22] K. Maki, Prog. Theor. Phys. **31**, 731 (1964).
[23] S. P. Chockalingam *et al.*, Phys. Rev. B **77**, 214503 (2008).